

Estimation of Wave Drift Force by Numerical Wave Tank, 2nd Report

Katsuji Tanizawa, Makiko Minami, Hiroshi Sawada
 Ship Research Institute, Tokyo, Japan

Shigeru Naito
 Osaka University, Osaka, Japan

ABSTRACT

A linear and a fully nonlinear numerical wave tanks (NWTs) were applied to study wave drift force acts on a two-dimensional Lewis form body in finite depth wave flume. These NWTs are based on potential theory and the fluid and floating body motions are directly simulated in time domain. Boundary value problems both on the velocity potential ϕ and its time derivative $\partial\phi/\partial t$ are solved at each time step. The coupling condition between fluid and floating body is imposed as the implicit boundary condition of $\partial\phi/\partial t$ on wetted body surface. The radiation condition at both tank ends are satisfied by artificial damping technique. Using these NWTs, effects of the floor step of the flume on wave drift force were studied. Measurement of wave drift force was also conducted in our two dimensional wave flume. In this second report, the results of simulations and measurements are presented and the effect of the floor step on wave drift force is discussed.

KEY WORDS : Wave drift force, Sea floor step, Numerical wave tank

INTRODUCTION

A joint research project named “On the drifting prevention of disabled ships in rough waves” is conducted by Ship Research Institute, Maritime Safety Agency, Osaka University, Kyushu University, rope manufactures and a salvage company. In this project, a prototype onboard towing support system for rescue ships is expected to be developed as a final output. As a part of this project, the authors are studying wave drift force and drift motion of a freely floating body under various conditions. Shape of the sea floor is one of the important condition. When a disabled ship is drifting to coast and be in danger of running aground, accurate estimation of required power for rescue ships as well as estimation of drifting speed and course is very important to avoid disaster. The floor shape effect should be considered to estimate accurate wave drift force at the shallow seas.

Wave drift force is one of the old topics in marine hydrodynamics. In the early years of the research, Maruo (1960) investigated the mechanism of wave drift force from the conservation law of en-

ergy and momentum of wave field around a floating body. Newman (1967) derived wave drift force and steady vertical moment for a freely floating ship and computed them for a Series 60 hull form. Nojiri and Murayama (1975) extended Maruo’s theory to shallow water and validated it by two dimensional experiment. Kudo and Kobayashi (1977,1978) studied wave drift force on sphere and spheroid. After these works, many researchers and engineers applied these theories to ships and ocean structures.

Following these study, the authors selected a step as the simplest shape of the coastal sea floor and studied its effect on wave drift force theoretically, experimentally and numerically. For this basic study, a two dimensional Lewis form body was used as a floating body. At the previous ISOPE conference, the authors (1999) showed that wave drift force on this Lewis form body estimated by our fully nonlinear simulation method well agreed with the linear theory and measured value of Nojiri et al.(1975). Accordingly, we developed a linear time domain simulation method as a fast simulator of radiation-diffraction problem and used it for parameter study.

THEORETICAL RELATION AMONG WAVES AND WAVE DRIFT FORCE

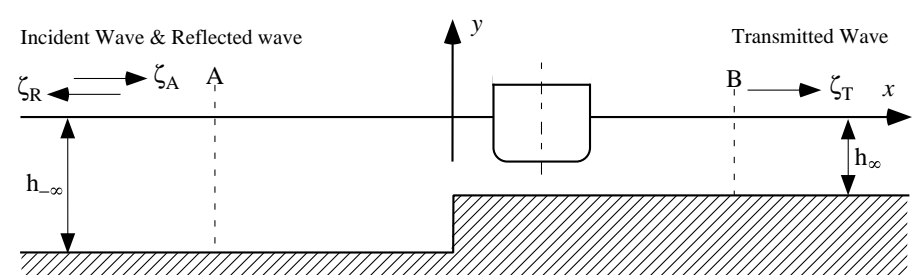


Figure 1 Wave flume with a floor step

Fig.1 shows a two dimensional wave flume with a floor step at $x = 0$. The depth of the flume at both sides of the step are $h_{-\infty}$ and h_{∞} respectively. Incident wave travels from $x = -\infty$ to ∞ . Part of wave energy is reflected by step and floating body and the rest is transmitted to $x = \infty$. In this study, we assume ideal fluid and no energy dissipation by floating body. We focus our attention only on the periodically steady state. Therefore, the height of

incident wave : ζ_A , reflected wave : ζ_R and transmitted wave : ζ_T are constant in time and space.

The wave energy E is a function of wave amplitude ζ and independent of water depth h ;

$$E = \frac{1}{2}\rho g\zeta^2 . \quad (1)$$

However its propagation speed is the group velocity V which depends on water depth;

$$V = V_c n , \quad (2)$$

$$V_c = \frac{\omega}{k} , \quad (3)$$

$$n = \frac{1}{2} \left(1 + \frac{2kh}{\sinh 2kh} \right) , \quad (4)$$

where V_c is the phase velocity of wave, ω and k are wave frequency and wave number respectively and n is ratio between group velocity and phase velocity.

Then conservation law of wave energy in the region between the control surface A and B can be written as

$$(E_A - E_R)V_{-\infty} = E_TV_{\infty} , \quad (5)$$

where E_A, E_R and E_T are energy of incident, reflected and transmitted waves and $V_{\pm\infty}$ are group velocity at $x = \pm\infty$ respectively. In the following part of this paper, variables with subscript $\pm\infty$ means the values at $x = \pm\infty$. Substituting (1) ~ (4) into (5), we have following relation

$$\frac{n_{-\infty}}{k_{-\infty}}(\zeta_A^2 - \zeta_R^2) = \frac{n_{\infty}}{k_{\infty}}\zeta_T^2 . \quad (6)$$

It is known that wave drift force F_D is obtained from reflected wave amplitude as

$$F_D = n_{-\infty}\rho g\zeta_R^2 . \quad (7)$$

Substituting (6), the theoretical relation among waves and wave drift force is obtained. They are

$$\frac{F_D}{\frac{1}{2}\rho g\zeta_A^2} = 2n_{-\infty} \left(\frac{\zeta_R}{\zeta_A} \right)^2 \quad (8)$$

$$= n_{-\infty} \left\{ 1 + \left(\frac{\zeta_R}{\zeta_A} \right)^2 \right\} - n_{\infty} \frac{k_{-\infty}}{k_{\infty}} \left(\frac{\zeta_T}{\zeta_A} \right)^2 \quad (9)$$

$$= 2n_{-\infty} \left\{ 1 - \frac{k_{-\infty}}{k_{\infty}} \frac{n_{\infty}}{n_{-\infty}} \left(\frac{\zeta_T}{\zeta_A} \right)^2 \right\} . \quad (10)$$

OUTLINE OF THE NUMERICAL SIMULATION

Fully Nonlinear Numerical Wave Tank

We considered a two dimensional wave flume bounded by free-surfaces S_f , wave making vertical boundary S_w at left side, flume floor with a step and rigid vertical wall at right side S_b and floating body surface S_s . Here, the gravitational acceleration g , the fluid density ρ and the length of incident regular wave λ are chosen as units to nondimensionalize the problem. A space-fixed Cartesian coordinate system $o-xz$ is used, with x coincident with the calm free-surface and z positive upward. The fluid is assumed to be homogeneous, incompressible, inviscid and its motion irrotational. The fluid motion can be described by the

velocity potential ϕ and its time derivative $\partial\phi/\partial t \equiv \phi_t$. In the fluid domain, ϕ and ϕ_t satisfy Laplace's equation

$$\nabla^2\phi = \nabla^2\phi_t = 0 . \quad (11)$$

Green's second identity can be applied on both ϕ and ϕ_t

$$c(\mathcal{Q}) \left\{ \begin{array}{l} \phi(\mathcal{Q}) \\ \phi_t(\mathcal{Q}) \end{array} \right\} = \int_S \left\{ \begin{array}{l} \phi(\mathcal{P}) \\ \phi_t(\mathcal{P}) \end{array} \right\} \frac{\partial}{\partial n} \ln r(\mathcal{P}, \mathcal{Q}) \\ - \ln r(\mathcal{P}, \mathcal{Q}) \left\{ \begin{array}{l} \frac{\partial\phi(\mathcal{P})}{\partial n} \\ \frac{\partial\phi_t(\mathcal{P})}{\partial n} \end{array} \right\} dS , \quad (12)$$

where \mathcal{P}, \mathcal{Q} are points on the boundary, n is the outward normal direction of the boundary, $r(\mathcal{P}, \mathcal{Q})$ is the distance between \mathcal{P} and \mathcal{Q} , $c(\mathcal{Q})$ represents the angle subtended at \mathcal{Q} by boundaries.

On the wave making boundary S_w , the flux of linear propagating wave is imposed as the boundary condition.

$$\frac{\partial\phi}{\partial n} = -\frac{k\zeta_A \cosh k(z+h)}{\omega \cosh kh} \cos(kx - \omega t) \quad (13)$$

$$\frac{\partial\phi_t}{\partial n} = -\frac{k\zeta_A \cosh k(z+h)}{\cosh kh} \sin(kx - \omega t) \quad (14)$$

Where k, ω and ζ_A are wave number, angular frequency and wave amplitude of the incident wave, respectively.

On the free-surface, kinematic and dynamic free-surface boundary conditions,

$$\frac{D\phi}{Dt} = -z + \frac{1}{2}(\nabla\phi)^2 - \nu(x_e)(\phi - \phi_e) \quad (15)$$

$$\frac{D\mathbf{x}}{Dt} = \nabla\phi - \nu(x_e)(\eta - \eta_e) , \quad (16)$$

are imposed, where η is the wave elevation and $\nu(x_e)$ is the damping coefficient

$$\nu(x) = \begin{cases} \alpha\omega\left(\frac{x-x_0}{\lambda}\right)^2, & \text{for } x_0 \leq x \leq x_1 = x_0 + \beta\lambda \\ 0, & \text{for } x < x_0 \text{ or } x > x_1 \end{cases} . \quad (17)$$

The artificial damping terms added to dynamic and kinematic free-surface boundary conditions are effective only inside of damping zones. (Cointe et.al. 1990) The performance of this damping zone is controlled by two parameters α and β . α is used to control the strength of damping and β is used to control the length of damping zone. ϕ_e, η_e are reference values. This damping zone absorbs differences $\phi - \phi_e$ and $\eta - \eta_e$. When the damping zone is placed in front of a rigid wall and works as a simple absorber, the reference values are set to $\phi_e = 0, \eta_e = 0$. On the other hand, when the damping zone is placed in front of a wave making boundary, the reference values are set to

$$\phi_e = \frac{\zeta_A \cosh k(h+z)}{\omega \cosh kh} \sin(kx - \omega t) , \quad (18)$$

$$\eta_e = \zeta_A \cos(kx - \omega t) . \quad (19)$$

The wave reflection coefficient of this damping zone is less than 2%, when the tuning parameters are appropriately set to $\alpha = \beta = 1$ for a regular wave.

On the body surface, impermeability condition with respect to ϕ is expressed as

$$\frac{\partial\phi}{\partial n} = \mathbf{n} \cdot (\mathbf{v}_0 + \boldsymbol{\omega} \times \mathbf{r}) , \quad (20)$$

where \mathbf{v}_o and $\boldsymbol{\omega}$ are translating and angular velocities of the body, respectively.

Boundary condition on the body surface with respect to ϕ_t is given as

$$\begin{aligned} \frac{\partial \phi_t}{\partial n} = & -k_n (\nabla \phi - \mathbf{v}_o - \boldsymbol{\omega} \times \mathbf{r})^2 + \mathbf{n} \cdot (\dot{\mathbf{v}}_o + \dot{\boldsymbol{\omega}} \times \mathbf{r}) \\ & + \mathbf{n} \cdot \boldsymbol{\omega} \times (\boldsymbol{\omega} \times \mathbf{r}) + \mathbf{n} \cdot 2\boldsymbol{\omega} \times (\nabla \phi - \mathbf{v}_o - \boldsymbol{\omega} \times \mathbf{r}) \\ & - \frac{\partial}{\partial n} \left(\frac{1}{2} (\nabla \phi)^2 \right), \end{aligned} \quad (21)$$

where k_n is curvature of body surface, $\dot{\mathbf{v}}_o, \dot{\boldsymbol{\omega}}$ are translating and angular accelerations of the body, respectively (Tanizawa, 1995).

On the floating body surface, $\dot{\mathbf{v}}_o$ and $\dot{\boldsymbol{\omega}}$ cannot be specified explicitly because they are functions of hydrodynamic pressure ϕ_t . However, using the equation of body motion, $\dot{\mathbf{v}}_o$ and $\dot{\boldsymbol{\omega}}$ can be eliminated and the implicit body surface boundary condition can be derived. Denoting the inertia tensor of a floating body as \mathbf{M} and the generalized normal vector of body surface as $\mathbf{N} = (\mathbf{n}, \mathbf{n} \times \mathbf{r})$, the implicit boundary condition is written as

$$\begin{aligned} \frac{\partial \phi_t}{\partial n} = & \mathbf{N} \mathbf{M}^{-1} \int_{S_s} -\phi_t \mathbf{N} ds \\ & + \mathbf{N} \mathbf{M}^{-1} \left\{ \int_{S_s} \left(-z - \frac{1}{2} (\nabla \phi)^2 \right) \mathbf{N} ds + \mathbf{F}_g \right\} \\ & + q - \frac{\partial}{\partial n} \left(\frac{1}{2} (\nabla \phi)^2 \right), \end{aligned} \quad (22)$$

where \mathbf{F}_g is the sum of gravity, mooring force and other external forces acting on the body and q is the term which can be explicitly evaluated from the solution of the velocity field as

$$\begin{aligned} q = & -k_n (\nabla \phi - \mathbf{v}_o - \boldsymbol{\omega} \times \mathbf{r})^2 \\ & + \mathbf{n} \cdot \boldsymbol{\omega} \times (\boldsymbol{\omega} \times \mathbf{r}) + \mathbf{n} \cdot 2\boldsymbol{\omega} \times (\nabla \phi - \mathbf{v}_o - \boldsymbol{\omega} \times \mathbf{r}). \end{aligned} \quad (23)$$

With these boundary conditions and Green's second identity with respect to ϕ and ϕ_t , both the velocity and acceleration fields can be solved numerically by means of BEM. The solutions are integrated with respect to time by the 4th order Runge-Kutta method, then the fluid and body motions are simulated in the time domain. Free-surface is traced by the Mixed Eulerian and Lagrangian method (MEL).

Linear Numerical Wave Tank

Linear NWT is almost identical to the fully nonlinear NWT except boundary conditions. In the linear simulation, free-surface boundary conditions (15,16) are linearized as

$$\frac{\partial \phi}{\partial t} = -z - \nu(x_e)(\phi - \phi_e) \quad (24)$$

$$\frac{dz}{dt} = \frac{\partial \phi}{\partial z} - \nu(x_e)(\eta - \eta_e), \quad (25)$$

and body surface boundary condition for ϕ_t (21) as well as the implicit body surface boundary condition (22) are linearized as

$$\frac{\partial \phi_t}{\partial n} = \mathbf{n} \cdot (\dot{\mathbf{v}}_o + \dot{\boldsymbol{\omega}} \times \mathbf{r}) \quad (26)$$

and

$$\frac{\partial \phi_t}{\partial n} = \mathbf{N} \mathbf{M}^{-1} \left\{ \int_{S_s} (-\phi_t - z) \mathbf{N} ds + \mathbf{F}_g \right\}, \quad (27)$$

respectively. By this linearization, the boundary shape is fixed to the mean position of harmonic oscillation and this makes the speed of linear simulation much faster than fully nonlinear simulation. This linear simulation method is as accurate as frequency

domain methods, at the same time flexible to apply various linear problems.

Both in the nonlinear and linear methods, simulations are started from the calm condition and continued until body motions and wave field are converged to the periodically steady state.

EXPERIMENT

Table 1 Principle Dimensions

Breadth	B	0.40	m
Draft	d	0.20	m
Lewis form parameter	H_0	1.00	
	σ	1.00	
Metacenter height	GM	0.055	m
Displacement/Length	W	80.0	kg/m
Radius of gyration	$\sqrt{I_{yy}/W}$	0.13	m
Natural roll period	T_r	1.23	sec

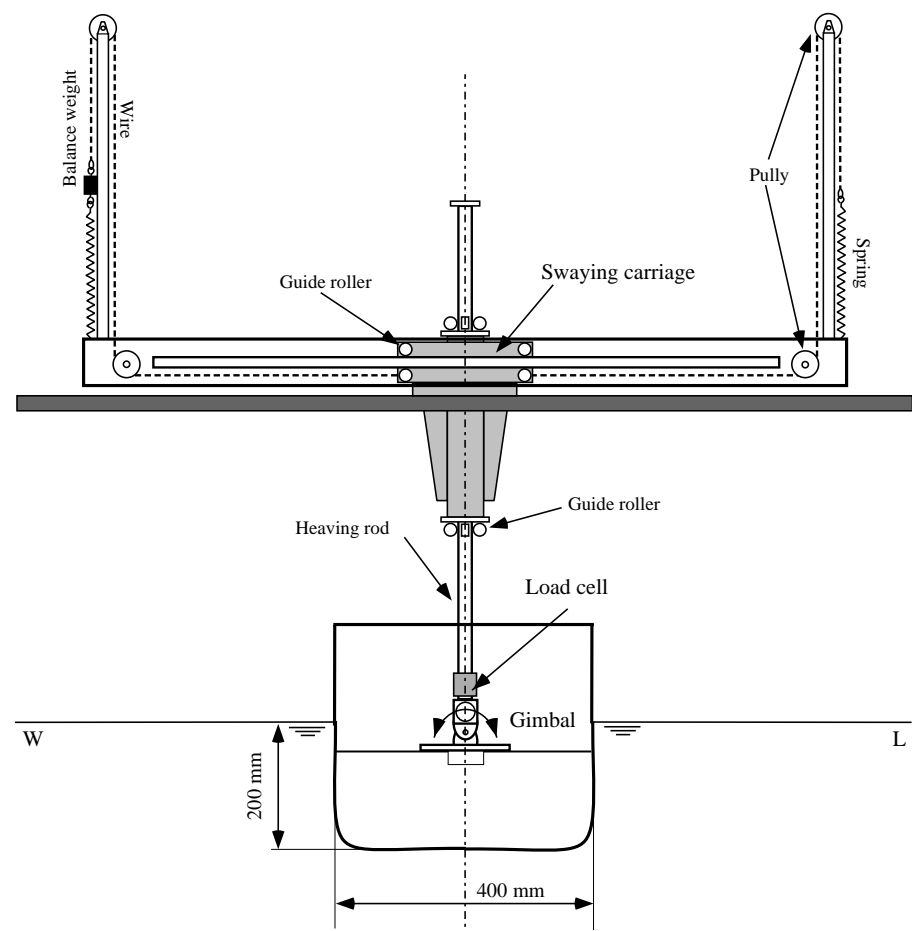


Figure 2 Floating Body and Measuring Equipment

2-D Wave Flume

Experiment was conducted at a two dimensional wave flume of Ship Research Institute. The length and width of the flume is 26 m and 0.5 m respectively. On the right half of the floor, a rigid raised floor was installed to form a step. The step height was 0.2 m. The depth of water was set to 0.5 m at the left half part, therefore that of the right half part on the step was 0.3 m. The entrance of raised floor was covered so that no wave energy travels under it. This wave flume is equipped with an absorbing wave maker at one end and a wave breaking beach at another end. The energy absorbing efficiency of the wave maker somewhat depends on frequency but 95% in average. This value is good enough to achieve periodically steady wave field including multiple reflection between the wave maker and floating body. Wave elevation was measured by six electric capacity type wave probes. Goda's method (1976) is used to decompose the incident and reflected waves from measured wave elevation.

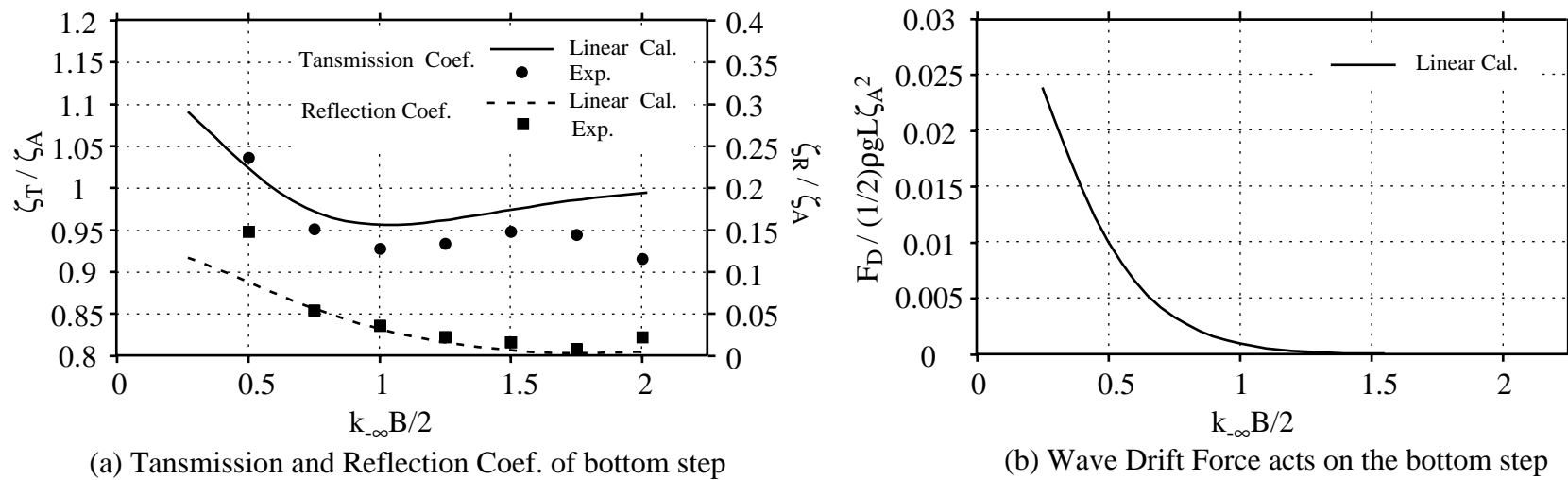


Figure 3 Wave reflection, transmission and drift force by the floor step itself

Floating Body and Measuring Equipment

A Lewis form 2-D model was used for this study. The body was attached to a motion measuring equipment and moored by weak springs only in horizontal direction. Measured items are free motions (Sway, Heave, Roll) and wave drift force. Table 1 and Fig.2 show the principle dimensions and section shape of the body with measuring equipment, respectively. Wave drift force is directly measured by the load cell attached at the low end of the heaving rod. The time averaged value of the measured horizontal force is wave drift force.

RESULTS

In figures of this paper, the results of the linear simulation are drawn by lines and the results of the experiment and fully nonlinear simulation are plotted using symbols.

Wave Drift Force on the Floor Step Itself

To obtain wave drift force acts on the floor step itself, the wave field without floating body was measured. Fig.3(a) shows measured and simulated transmission and reflection coefficients of the floor step. Horizontal axis is nondimensional wave number $k_{-\infty} B/2$, where a half of the floating body width $B/2 = 0.2m$ is used as the principle length. Agreement between measured and simulated reflection coefficient is good in general. At short wave range, ($k_{-\infty} B/2 > 1.5$), the measured transmission coefficients are lower than simulated line. This is due to weak wave breaking above the floor step. On the other hand, at long wave range ($k_{-\infty} B/2 < 0.5$), both measured and simulated wave transmission coefficients exceed one. If water depth is uniform, this can not be happen. However as (6) means, if water depth is different at $x_{\pm\infty}$, wave transmission coefficient can be larger than one. The result of linear simulation satisfies (6) and also shows good agreement with measured data. Substituting the simulated reflection coefficient into (8), wave drift force on the floor step can be estimated as shown in Fig.3(b). Wave drift force on the floor step itself was found to be very small even in long wave range.

Wave Drift Force on the Floating Body

In this study, wave number and the relative location of the floating body to the floor step were chosen as main parameters of wave

drift force. However, due to the restriction of measuring appliance, we conducted the experiment only for three different locations. The first location was just above the step ($x = 0m$), next location was the one meter weather side of the step ($x = -1m$) and the last location was one meter lee side of the step ($x = 1m$). To study detailed dependency of wave drift force to the relative location, the linear simulation was applied.

Fig.4 shows comparison among measured and estimated values by fully nonlinear and linear simulation for $x = 0m$. Using balancing weights, mean position of the center-line of the body was roughly kept just above the floor step during the measuring. Also in fully nonlinear simulations, horizontal constant force and weak mooring force, which is proportional to the horizontal displacement, were applied to keep the mean position at $x = 0m$. Fig.4 (a,b,c) show amplitude and phase of floating body motions. Overall, simulated motions well agree with measured motions. Fig.4(d,e) show reflection and transmission coefficients of wave. In the short wave range, simulated reflection coefficient is larger than measured value. This is due to weak wave breaking near the intersection line of free-surface and body surface at the weather side. On the other hand, simulated transmission coefficient well agrees with measured values. Fig.4(f) shows wave drift force acts on the body. The agreement among measured values and simulated values is good. Wave drift force was directly measured by the load cell attached between heaving-rod and gimbal of the measuring equipment. Simulated values were obtained from reflection and transmission coefficients using (9). From the total wave drift force obtained from (9), wave drift force acts on the floor step itself, fig.3(b), was subtracted assuming that the cross-component of wave drift force due to the interaction between the step and floating body is negligible. We can estimate wave drift force directly from the pressure integral on the wet body surface. However, as we reported at the previous ISOPE conference (1999), simulated steady pressure component by our NWTs are not accurate enough to estimate wave drift force. The cause of this inaccuracy only in steady component is still not clear. Therefore also in this paper, we estimated wave drift force from wave field far from the body. As fig.4 shows the fully nonlinear simulation gives almost the same results as linear simulation. This means that wave drift force is proportional to the square of the wave amplitude and higher order effects are no so significant even in steep wave unless wave is breaking. The linear simulation is considered to be good enough for the estimation wave drift force.

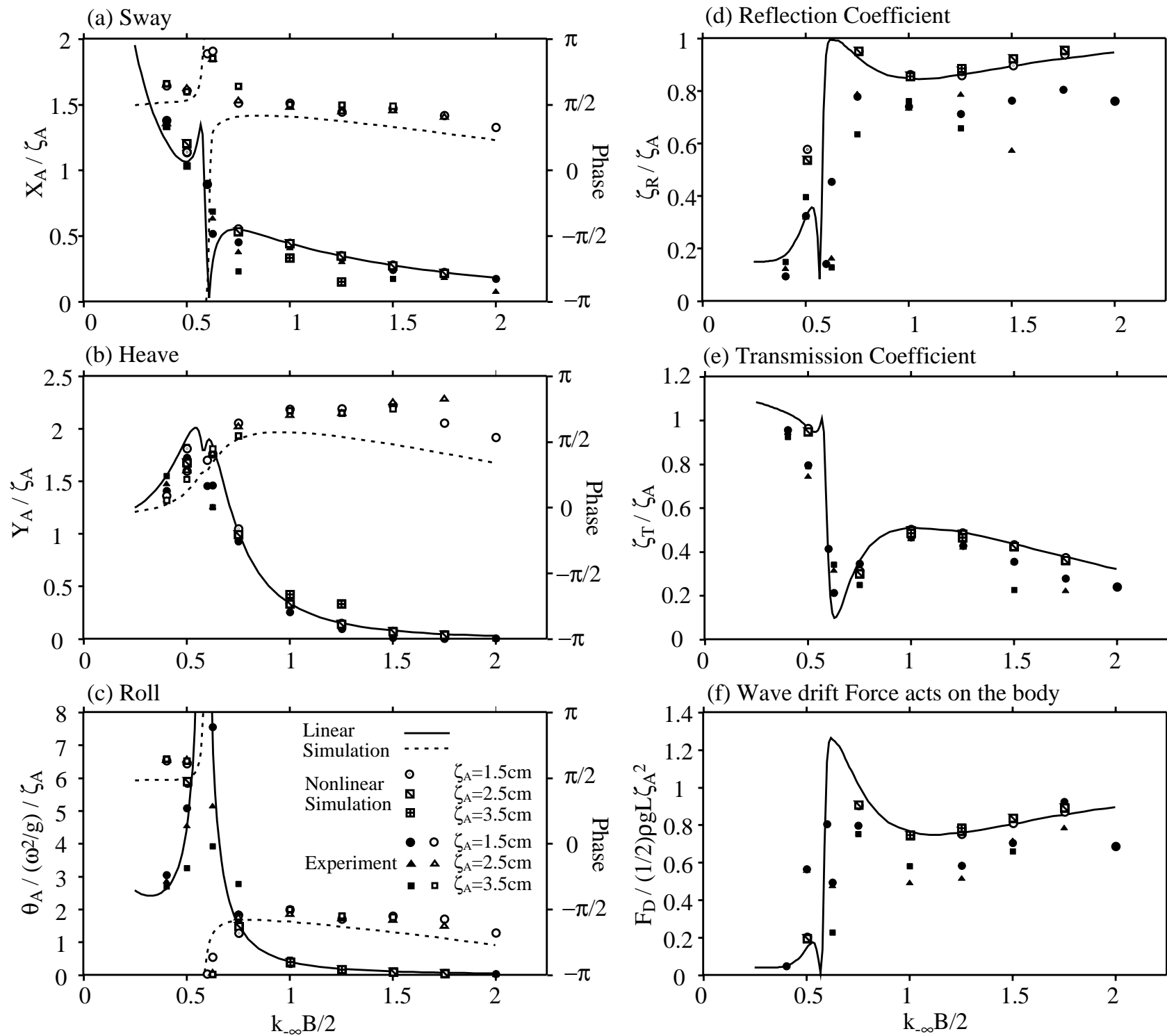


Figure 4 Floating body motions, wave reflection and transmission coefficients and wave drift force at $x = 0m$.

Fig.5 and Fig.6 show the same comparison for $x = -1m$ and $x = 1m$, respectively. Only the linear simulation was applied for these two cases. Agreement between measured values and simulated values are also good, overall. From these comparison shown in fig.4,5,6, we consider that the simulated wave drift force is reliable.

The effect of floor step on wave drift force was studied more precisely by the linear simulation. Fig.7 shows the simulated wave drift force acts on the body as a function of the location. The horizontal axis is distance between the center line of the body and the floor step. Its range is $\lambda_{-\infty} \leq x \leq \lambda_{\infty}$, where $\lambda_{\pm\infty}$ are wave lengths at the both sides of the floor step. In case of the wave frequency $\omega = 4.772$ rad/sec, wave drift force significantly increases when the body enters in the shallower area. Oscillation of wave drift force is also observed. The lengths of this oscillation are equal to $\lambda_{\pm\infty}/2$. On the other hand, in case of the wave frequency $\omega = 5.345$, rad/sec, change and oscillation of wave drift force are not so significant.

Fig.8 shows the entire picture of wave drift force as a function of wave number $k_{\infty}B/2$ and the location kx . This figure clearly shows that the effect of floor step is significant in long wave range $k_{\infty}B/2 < 0.6$ and shallower area $x > 0$. In this wave range and area, wave drift force oscillates and shows some local peaks. However they are lower than the ridgeline behind them. The ridgeline at the roll resonant frequency (heave resonant frequency is also near in this calculation) forms the highest peak. The slope of longer wave range from the ridgeline is very steep but the that of shorter wave range is gentle and almost no effect of floor step is observed.

CONCLUSION

Linear and fully nonlinear numerical wave tanks were applied to estimate wave drift force on a two dimensional floating body and the effect of floor step on wave drift force was studied numerically, theoretically and experimentally. Following items are main conclusions of this study.

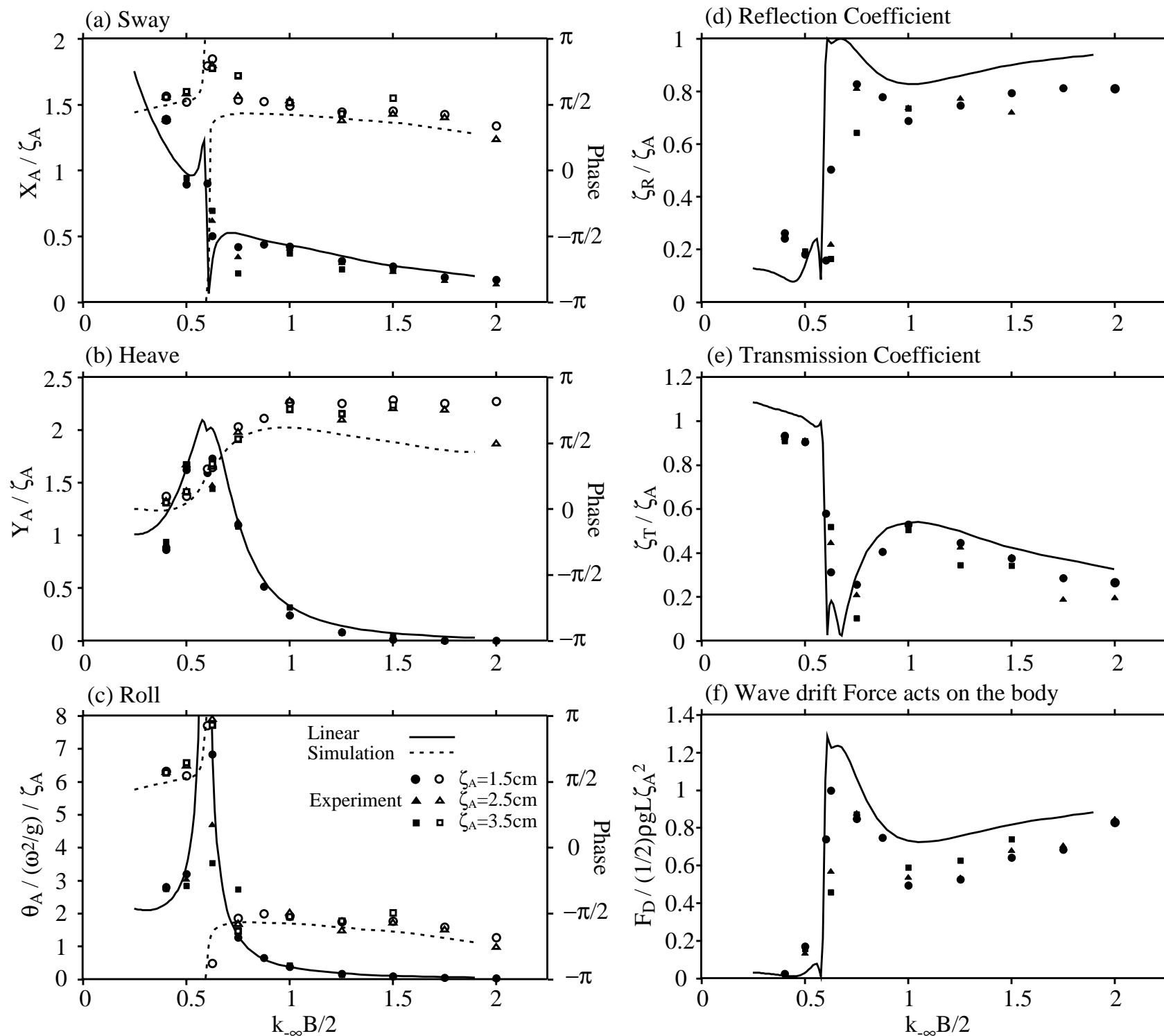


Figure 5 Floating body motions, wave reflection and transmission coefficients and wave drift force at $x = -1m$.

1. The linear theoretical relations among incident wave, reflected wave, transmission wave and wave drift force were obtained considering the difference of water depth at both far ends of the wave flume ($x = \pm\infty$).
2. A linear time domain simulation code was developed as a fast simulation method and used for the parameter study of wave drift force.
3. Simulated motions and wave field by the linear code as well as the fully nonlinear code agreed with measured values in overall.
4. Agreement between measured and simulated wave drift forces was also good.
5. The effect of floor step is significant only in long wave range $k_{\infty}B/2 < 0.6$ and shallower area on the step $x > 0$.

For more detailed analysis of floor step effect on wave drift force, we have to improve the accuracy of NWT for the computation of steady pressure component on floating body surface. In general, the steady pressure component is small and the accuracy of numerical calculation is lower than that of first order component.

However, the second and third order oscillating pressure components simulated by our fully nonlinear NWT was proved to be as accurate as other NWTs (Tanizawa and Clément, 2000). We are seeking the essential cause by investigating our NWT code down to the minutes details.

REFERENCE

- Maruo,H. (1960) "The drift of a body floating on waves", *J.S.R.*, Vol.4, No.3
- Newman,J.N. (1967) "The drift force and moment on ships in waves", *J.S.R.*, Vol.11, No.1
- Nojiri,N. and Murayama,K. (1975) "A study on the drift force on two dimensional floating body in regular waves" *Trans. West-Japan Soc. Nav. Arch.*, Vol.51
- Kudo,K. and Kobayashi,K. : The drifting force acting on a three-dimensional body in waves (1st & 2nd report), *J. Soc. Nav. Arch. Japan*, vol.141 & 144, (1977,1978)

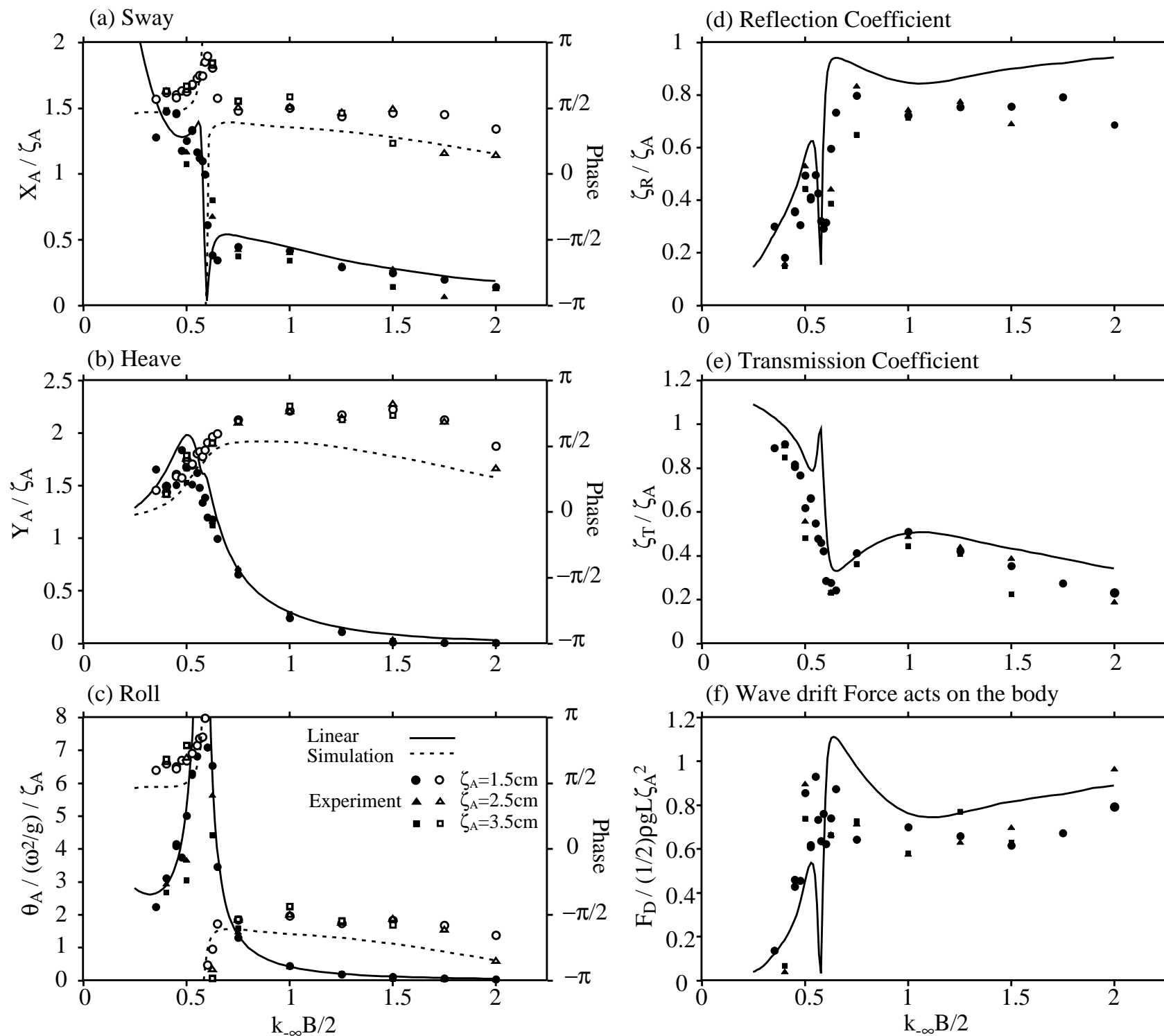


Figure 6 Floating body motions, wave reflection and transmission coefficients and wave drift force at $x = 1m$.

Goda, Y., Suzuki, Y., Kishira, Y. and Kikuchi, O. (1976) "Estimation of incident and reflected waves in random wave experiments" *Rept. Port and Harbour Res. Inst.*, vol.248, pp3-24

Cointe, R., Geyer, P., King, B., Molin, B. and Tramon, M. (1990), "Nonlinear and linear motions of a rectangular barge in perfect fluid", *Proc. of the 18th Symp. on Naval Hydro., Ann Arbor, Michigan*, pp85-98

Tanizawa, K. (1995) "A Nonlinear Simulation Method of 3-D Body Motions in Waves", *J. Soc. Nav. Arch. Japan*, Vol.178, pp179-191

Kashiwagi, M. (1996) "Full-nonlinear simulation of hydrodynamic forces on a Heaving two-dimensional body" *J. Soc. Nav. Arch. Japan*, Vol.180

Tanizawa, K. (1996) "Long time fully nonlinear simulation of floating body motions with artificial damping zone", *J. Soc. Nav. Arch. Japan*, Vol.180, pp311-319

Tanizawa, K. and Naito, S. (1997) "A study on parametric roll motions by fully nonlinear numerical wave tank", *Proc. of 11th ISOPE Conf., Honolulu, Hawaii*, Vol.3, pp69-75

Tanizawa, K., Minami, M. and Naito, S. (1999) Estimation of wave drift force by numerical wave tank *Proc. 9th ISOPE Conf.*, vol.3, Brest

Tanizawa, K. and Clément, A (2000) The report of NWT workshop *Proc. 10th ISOPE Conf.*, vol.3, Seattle

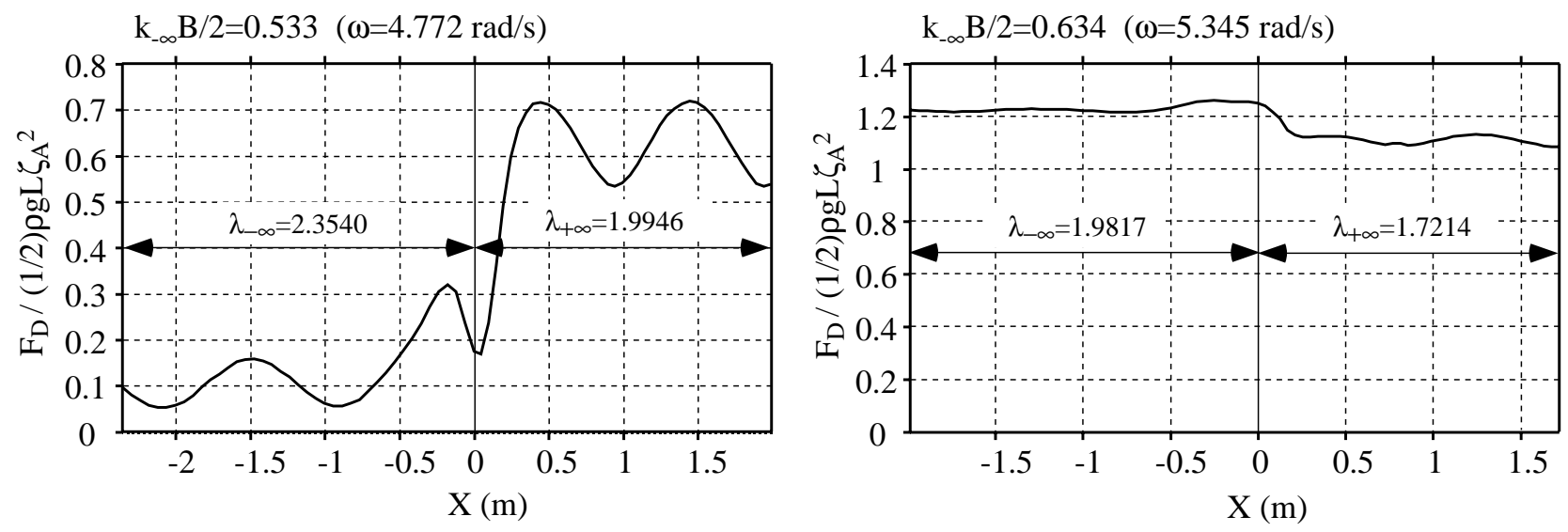


Figure 7 Wave drift force as a function of relative location of the body to the floor step

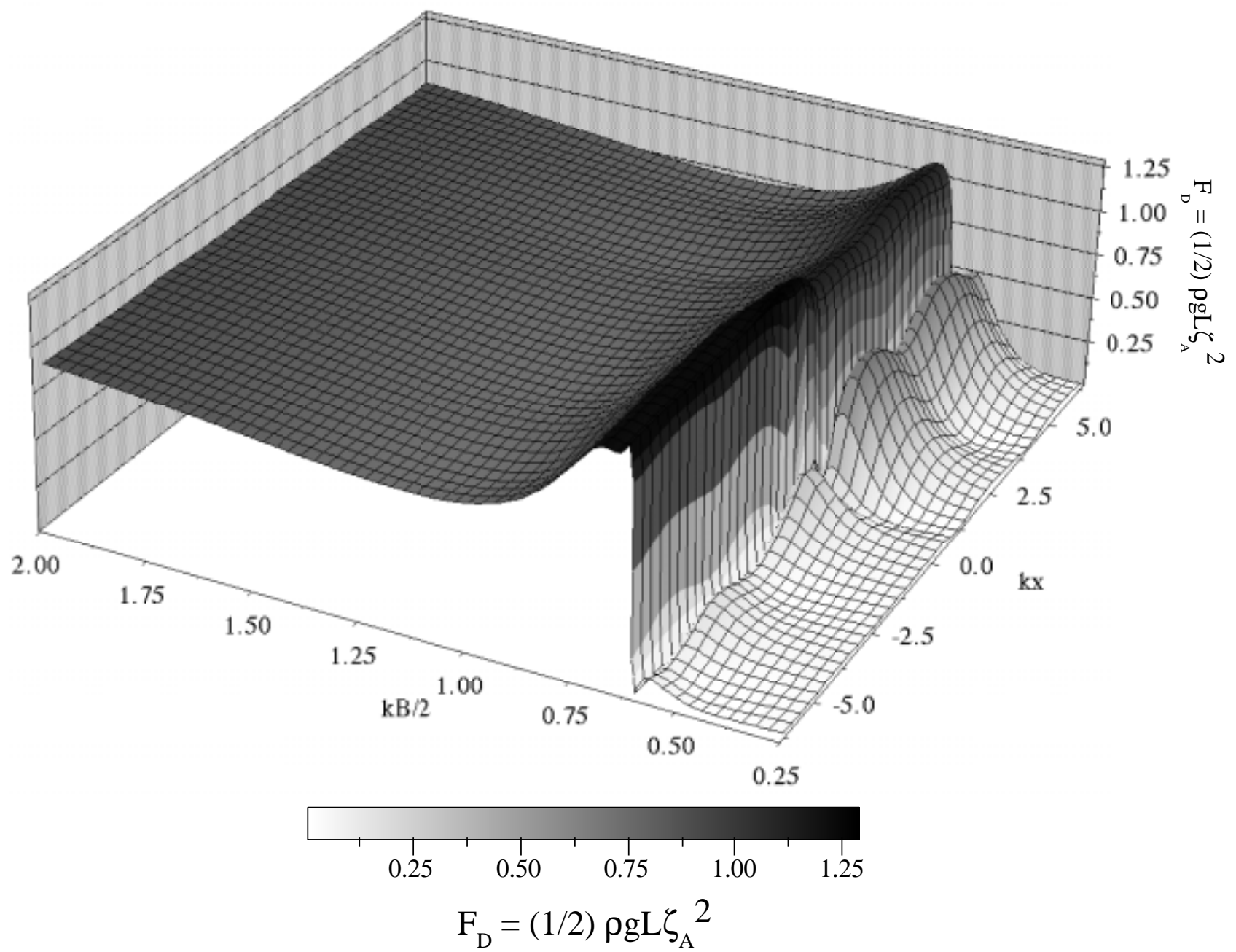


Figure 8 Wave drift force as a function of wave number and relative location of the body to the floor step